

This article was downloaded by:

On: 14 January 2011

Access details: *Access Details: Free Access*

Publisher *Taylor & Francis*

Informa Ltd Registered in England and Wales Registered Number: 1072954 Registered office: Mortimer House, 37-41 Mortimer Street, London W1T 3JH, UK



## **Molecular Simulation**

Publication details, including instructions for authors and subscription information:

<http://www.informaworld.com/smpp/title~content=t713644482>

### **Molecular dynamics simulation of shell-symmetric Pd nanoclusters**

Y. Pan<sup>a</sup>; S. Huang<sup>a</sup>; Z. Liu<sup>a</sup>; W. Wang<sup>a</sup>

<sup>a</sup> Key Lab for Nanomaterials, Division of Molecular and Materials Simulation, Ministry of Education, Beijing University of Chemical Technology, Beijing, People's Republic of China

**To cite this Article** Pan, Y. , Huang, S. , Liu, Z. and Wang, W.(2005) 'Molecular dynamics simulation of shell-symmetric Pd nanoclusters', *Molecular Simulation*, 31: 14, 1057 – 1061

**To link to this Article:** DOI: 10.1080/08927020500449401

**URL:** <http://dx.doi.org/10.1080/08927020500449401>

PLEASE SCROLL DOWN FOR ARTICLE

Full terms and conditions of use: <http://www.informaworld.com/terms-and-conditions-of-access.pdf>

This article may be used for research, teaching and private study purposes. Any substantial or systematic reproduction, re-distribution, re-selling, loan or sub-licensing, systematic supply or distribution in any form to anyone is expressly forbidden.

The publisher does not give any warranty express or implied or make any representation that the contents will be complete or accurate or up to date. The accuracy of any instructions, formulae and drug doses should be independently verified with primary sources. The publisher shall not be liable for any loss, actions, claims, proceedings, demand or costs or damages whatsoever or howsoever caused arising directly or indirectly in connection with or arising out of the use of this material.

# Molecular dynamics simulation of shell-symmetric Pd nanoclusters

Y. PAN, S. HUANG\*, Z. LIU and W. WANG

Key Lab for Nanomaterials, Division of Molecular and Materials Simulation, Ministry of Education, Beijing University of Chemical Technology, Beijing 100029, People's Republic of China

(Received October 2005; in final form October 2005)

The melting behaviour of Palladium (Pd) isolated shell-symmetric cubooctahedron and icosahedron nanoclusters, both consisting of 309 atoms, were simulated by Molecular Dynamics (MD) simulation, using the Sutton-Chen many-body potential (SC) for the interaction between the Pd atoms. The thermal, structural and dynamic properties were calculated for the Pd nanoclusters along the heating process. The cubooctahedron nanocluster melts around 1040 K, much lower than the melting point of bulk Pd system (1828.05 K). The icosahedron nanocluster melts around 1070 K. Furthermore, structural and dynamic evidence is found for the pre-melting of the nanoclusters. The outer two shells of the shell-symmetric nanocluster melt prior to their homogeneous melting of the whole nanoclusters.

During the last three decades, great interest has been shown in investigation of the melting behaviour of transition metallic clusters, both computationally and experimentally. Experiments on small metallic particles [1,2] show melting at considerably lower temperature than their bulk systems, suggesting that the melting process starts on the surface. However, whether surface melting is a phase transition separating from the overall melting cannot be explained by experiment itself. Earlier calculations on metallic clusters assumed that they were fragments of bulk solids such as face centred cubic (FCC) or body centred cubic (BCC) [3–5]. It was subsequently discovered that the clusters grow as polyhedra, which are made up of geometric shells of atoms, possessing five fold axes of symmetry, in particular [6–8]. These previous work has provided us better understanding on surface melting. However, no direct evidences on such phase transition have been reported.

In this paper, we investigated the heating process of a 309-atom Pd shell-symmetric cubooctahedron and icosahedron nanoclusters in molecular dynamics (MD) simulation, by the Sutton–Chen (SC) many-body potential [9,10]. The choice of Pd in this study is motivated by its rich applications in hydrogenation and dehydrogenation reactions. The SC potential has been well accepted to model different transition systems. Chan *et al.* [3] used SC potential to study transition metallic nanocluster. They found a convenient way to differentiate

the core atoms from the surface and near atoms. Wales *et al.* [6] used the SC potential to calculate global minima for transition metallic clusters with up to 80 atoms. They found that the likely global minimum of 55-atom cluster was Macky icosahedron, while the cubooctahedron is a near local minimum. Westergren *et al.* [7] investigated melting of Pd icosahedron nanoclusters of particular numbers of atoms in Monte Carlo (MC) simulation, by the tight-binding second momentum approximation (TB–SMA) potential. They found melting point of 309-atom Pd icosahedron nanocluster was 1121 K. In this work, the melting transition is identified through thermal properties calculation. Further structural and dynamic analysis provides direct evidences identifying surface melting transition separated from homogeneous melting of the nanoclusters.

All the MD simulations in this work were performed using the DL\_POLY programmes developed by Smith and Forester [11]. The MD equations of motion were integrated based on the Verlet leapfrog scheme [12]. The time step in all calculations was 1.0 fs, which led to quite stable dynamics trajectories for the system. The nanoclusters were isolated in a free space without the periodic boundary conditions. In this way, we simulated the nanoclusters in MD simulation with constant temperature ( $T$ ) for Berendsen thermostat, and constant atom number ( $N$ ). The nanoclusters were first relaxed for

\*Corresponding author. Email: huangsp@mail.buct.edu.cn

Table 1. Comparison of simulations of different running-time and time steps.

	5 K_cubooctahedron		5 K_icosahedron	
Time step/running time	1 fs/1 ns	0.5 fs/2 ns	1 fs/1 ns	0.5 fs/2 ns
$U$ (kJ/mol)	-348.985	-348.985	-350.203	-350.203
$C_V$ (kJ/mol K)	0.01775	0.017812	0.01773	0.01766
Cpu time(h)	8.98	37.12	9.29	37.16
	700 K_cubooctahedron		750 K_icosahedron	
Time step/running time	1 fs/1 ns	0.5 fs/2 ns	1 fs/1 ns	0.5 fs/2 ns
$U$ (kJ/mol)	-339.119	-339.182	-339.619	-339.806
$C_V$ (kJ/mol K)	0.02034	0.01933	0.01991	0.01904
Cpu time(h)	4.50	18.80	4.69	18.73

1000 ps at 5 K. Then, the cluster was heated from 5 K to over the melting temperature of 1400 K, with the fixed heating rate of 1 K/20 ps. For comparison, we reran the simulation using smaller time step (0.5 fs) and longer run (2 ns) at two temperature points for the cubooctahedron and icosahedron nanoclusters, respectively. The thermodynamic results between the original and the rerun simulations are listed in table 1. Since the results at very low temperature of 5 K are basically the same, and the results at higher temperature of 700 K only show slight differences, we chose 1.0 fs as the time step of the simulation, and 1 ns as running time.

Since the original cubooctahedron and icosahedron nanoclusters in this work are strictly shell-symmetric, we can take atom average of the structural and dynamic properties of the whole nanoclusters and the four shells, respectively. The shells segmentations are shown in table 2.

We define  $g_{cm}(r)$  as the pair correlation function around the centre of mass for the isolated cubooctahedron and icosahedron nanoclusters, which is given by

$$g_{cm}(r) = \frac{V}{N^2} \left\langle \sum_{i=1}^n \delta(\vec{r} - \vec{r}_i - \vec{r}_{cm}) \right\rangle \quad (1)$$

where  $N$  is the total atom number of whole nanoclusters (309 for this work),  $V$  is a settled volume of a large enough (assuring the isolation of the nanoclusters) cubic box with  $r_{cut}$  (12 Å for this work) in length,  $n$  is the atom number counted in for the particular shell or the whole cluster (309 for the whole nanoclusters, 192 for the fourth shell, etc.) and  $\vec{r}_{cm}$  is the coordinates of the centre of mass at each time step.

Accordingly, we define the shell-dependent, time-averaged atomic root mean square of displacement RMSD as

$$RMSD = \frac{\sum_i^n RMSD_i(dt)}{n} \quad (2)$$

where  $n$  is the atom number of the whole nanoclusters or the chosen shell,  $RMSD_i$  is the time-averaged root mean square of

displacement of atom  $i$ , given by

$$RMSD_i = \sqrt{\left\langle \sum_{t=0}^{T-dt} (r_i(t+dt) - r_i(t))^2 \right\rangle} \quad (3)$$

where  $r_i(t)$  is coordination of atom  $i$  at time of  $t$ ,  $T$  is the total time averaged, and  $dt$  is time lag of the working array.

To obtain  $g_{cm}(r)$  and RMSD, we averaged over a 200 ps trajectory at chosen temperatures. In particular, we used  $dt$  as 50 ps for the  $RMSD_i$  calculation.

The thermal properties of the Pd cubooctahedron and icosahedron nanoclusters are shown in figure 1. In figure 1(a) the potential energy  $U$  increases linearly under 900 K or over 1100 K. A rapid jump appears around the temperature range of 1040–1050 K, indicating the homogeneous melting. The  $C_V$ – $T$  curve shows the first

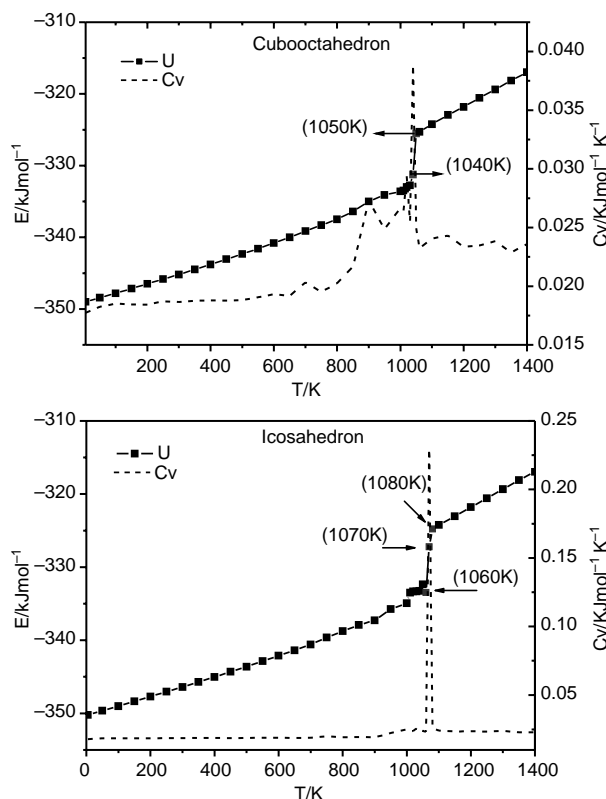


Figure 1. The temperature dependence of potential energy and isotonic heat capacity of Pd cubooctahedron and icosahedron nanoclusters along heating process. (a) Cubooctahedron and (b) Icosahedron.

Table 2. Atom number of each shell of the 309-atom cubooctahedron nanocluster.

	Centre	Shell 1	Shell 2	Shell 3	Shell 4	Total
Atom No.	1	12	42	92	162	309

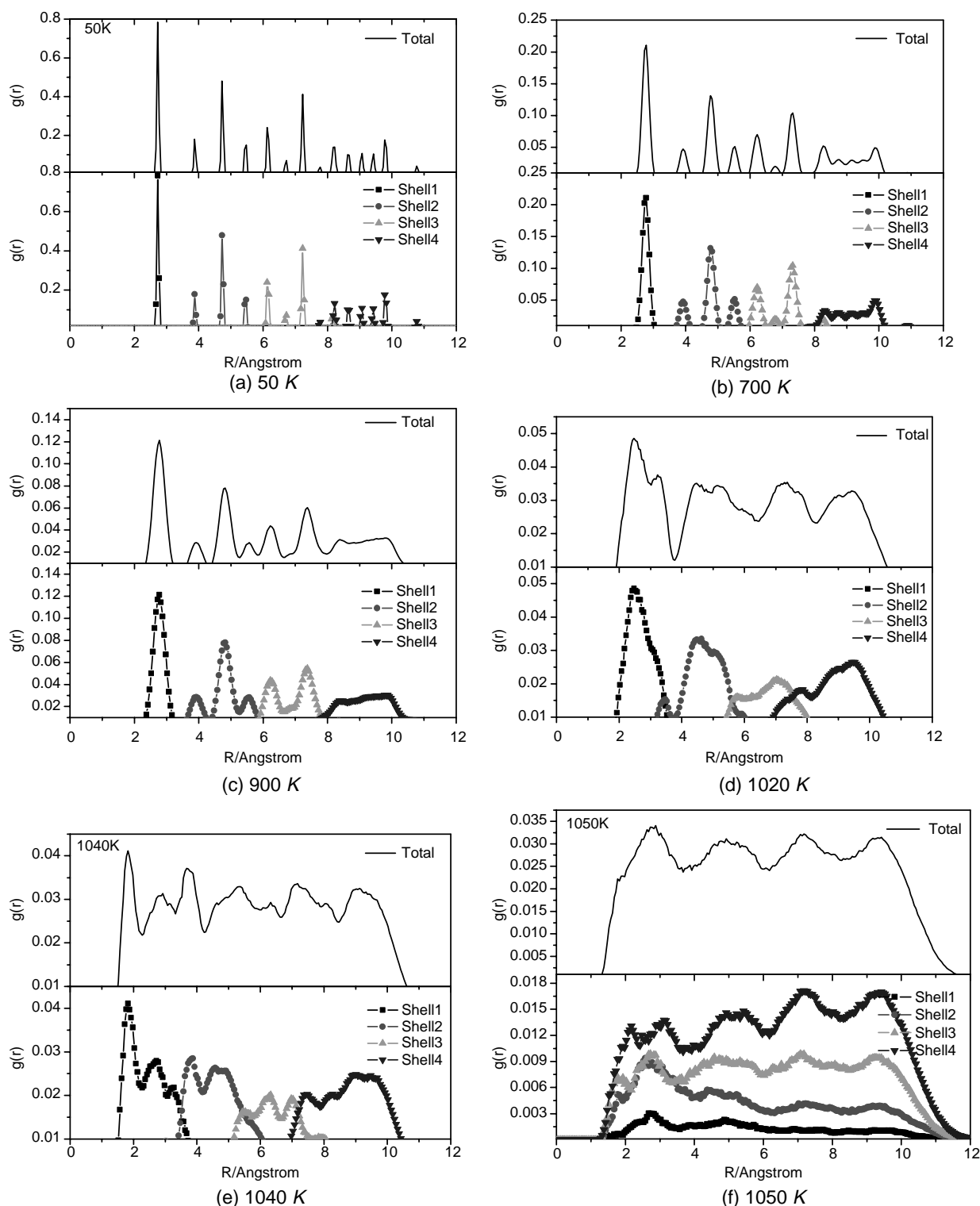


Figure 2. The whole and shells pair correlation function of Pd cubooctahedron nanocluster at different temperatures. (a) 50 K, (b) 700 K, (c) 900 K, (d) 1020 K, (e) 1040 K and (f) 1050 K.

observable peak at 700 K. Then the  $C_V$  ascends to a high value at 900 K, resulting in the apparent second peak. Combining with the structural and dynamic analysis below, we ascribe the first peak at 700 K to the Pd atoms getting activated, and the second peak at 900 K to the pre-melting. The maximum  $C_V$  peak appears at 1040 K.

Combined with the rapid jump in the  $U-T$  curve, it is found that the homogeneous melting happens around 1040 K. The melting point of the cubooctahedron nanocluster,  $T_{mc}$ , is defined as  $1040 \pm 10$  K. In figure 1(b) the potential energy  $U$  shows a rapid jump around temperature range of 1060–1080 K, indicating the

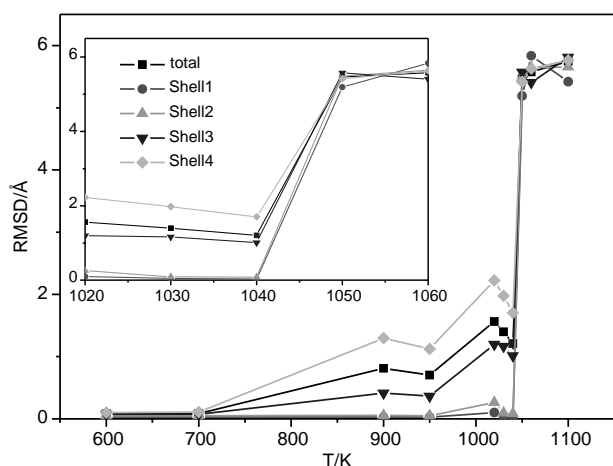


Figure 3. The temperature dependence of whole and shells root mean square of displacement of Pd cubooctahedron nanocluster.

homogeneous melting. The  $C_V$ - $T$  curve shows the first peak at 750 K (not obvious but observable). The second observable peak of the  $C_V$ - $T$  curve appears at 1000 K. Combining with the structural and dynamic properties, we consider that the icosahedron nanocluster gets activated at 750 K, and the pre-melting happens around 1000 K. The maximum  $C_V$  peak appears at 1070 K. Combined with the rapid jump in the  $U$ - $T$  curve, the melting point of icosahedron nanocluster,  $T_{mi}$ , is defined as  $1070 \pm 10$  K, which is consistent with Westergren's [7] simulation result (about 51 K (4.5%) lower than Westergren's). Therefore, it could be concluded that the SC potential and the TB-SMA potential have no distinct difference in generating melting point.

According to subtle information provided by the  $C_V$ - $T$  curve, we have generated MD simulation trajectories at several temperature points. The  $g_{cm}(r)$  and RMSD are calculated from these trajectories, and further evidences for pre-melting and homogeneous melting of the nanoclusters are obtained.

Figures 2(a)–(f) show the temperature dependence of the pair correlation function  $g_{cm}(r)$  of the whole Pd cubooctahedron nanocluster and its four shells. At the low temperature of 50 K, both the total and shells  $g_{cm}(r)$  present solid-like well-segregated sharp peaks. The shell- $g_{cm}(r)$  curves are clearly separated from each other, except for a slight intersection between the third and fourth shells. At 700 K, the total- $g_{cm}(r)$  maintains solid-like features. Peaks of the inner three shell- $g_{cm}(r)$  become lower and wider. The fourth shell- $g_{cm}(r)$  presents no segregated peaks. However, each peak is in the corresponding position of the segregated one in figure 2(a). This indicates that the fourth shell maintains a solid-like state, while it is highly activated. All the four shell- $g_{cm}(r)$  curves are still well separated at the edges. Up to 900 K, the inner two shell- $g_{cm}(r)$  curves show no peculiar changes in shape. The third shell- $g_{cm}(r)$  presents two major segregated peaks, while the other two little peaks disappear. The fourth shell- $g_{cm}(r)$  becomes a flat curve with no peaks. Combining with the apparent jump in  $C_V$ - $T$  curve at

900 K, the obvious change in the outer two shell- $g_{cm}(r)$  curves indicates the emergence of pre-melting on the surface of the Pd nanocluster. As yet, no further edge intersections between shell- $g_{cm}(r)$  are observed. At 1020 and 1040 K, both the total- $g_{cm}(r)$  and the shell- $g_{cm}(r)$ , loses solid-like features. Each shell- $g_{cm}(r)$  expands in  $R$ -direction, inward and outward. The edges between shell- $g_{cm}(r)$  become intersectant. The four shells are all highly activated and start to enter the liquid-field. At 1050 K, tremendous changes appear both in the total- $g_{cm}(r)$  and the shell- $g_{cm}(r)$ . The total- $g_{cm}(r)$  shows similar features of the liquid-like radial distribution function. It is a clear evidence for the whole nanocluster reaching homogeneous melting state. The borders between the shell- $g_{cm}(r)$  curves disappear completely, which means the Pd atoms of any shells can move freely within the whole nanocluster, either inward or outward. Therefore, the structural evidence for pre-melting of the nanocluster, starting at 900 K, is observed. The shell structure vanishing around 1050 K confirms the homogeneous melting, identified by the  $C_V$ - $T$  curve in figure 2.

Figure 3 shows the temperature dependence of the total- and shell- RMSD of the Pd cubooctahedron nanocluster. The total- and outer two shell-RMSD curves go up firstly at 900 K, which corresponds to the pre-melting behaviour of the nanocluster. The inner two shell-RMSD values are near zero up to 1040 K. This indicates that the inner two shells remain in the solid-like state before homogeneous melting. The total- and four shell-RMSD curves present significant increase in the temperature range of 1040–1050 K. All of the RMSD values reach the same high level at the temperatures over 1050 K. This confirms that the homogeneous melting happens around 1040 K.

In summary, by using the SC many-body potential [9,10] for the interaction between Pd atoms, we performed MD simulations of heating process of the 309-atom Pd shell-symmetric cubooctahedron and icosahedron nanoclusters. By calculating the structural and dynamic properties according to shell separation at chosen temperatures, surface melting is evidently observed. The outer two shells of the cubooctahedron and icosahedron nanoclusters start to melt at 900 and 1000 K, respectively, while the inner cores sustain solid-like state up to 1040 and 1070 K, respectively. The melting points of the two shell-symmetric nanoclusters are  $1040 \pm 10$  and  $1070 \pm 10$  K, respectively, which are much lower than that of the bulk system (1828.05 K from experiment). When homogeneous melting transition happens, the shell structure of the nanoclusters vanishes, and all the Pd atoms can move freely in the whole nanoclusters, either inward or outward.

### Acknowledgements

This work is financially supported by the National Basic Research Programme of China (Grant No.G2003CB615 807) and the National Natural Science Foundation of China (No. 20236010 and 20476004).

## References

- [1] Z.L. Wang, J.M. Petroski, T.C. Green, M.A. El-Sayed. Shape transformation and melting of cubic and tetrahedral platinum nanocrystals. *J. Phys. Chem. B*, **102**, 6145 (1998).
- [2] M. Schmidt, R. Kusche, E. Kronmüller, B.V. Issendorff, H. Haberland. Experimental determination of the melting point and heat capacity for a free cluster of 139 sodium atoms. *Phys. Rev. Lett.*, **79**, 99 (1997).
- [3] Y.H. Chui, K.Y. Chan. Analyses of surface and core atoms in a platinum nanoparticle. *Phys. Chem. Chem. Phys.*, **5**, 2869 (2003).
- [4] S.P. Huang, P.B. Balbuena. Melting of bimetallic Cu–Ni nanoclusters. *J. Phys. Chem. B*, **106**, 7225 (2002).
- [5] S.K.R.S. Sankaranarayanan, V.R. Bhethanabotla, B. Joseph. Molecular dynamics simulation study of the melting of Pd–Pt nanoclusters. *Phys. Rev. B*, **71**, 195415 (2005).
- [6] J.P.K. Doye, D.J. Wales. Global minima for transition metal clusters described by Sutton–Chen potentials. *New J. Chem.*, 733 (1998).
- [7] J. Westergren, S. Nordholm, A. Rosén. Melting of palladium clusters—Canonical and microcanonical Monte Carlo simulation. *Phys. Chem. Chem. Phys.*, **136**(5), 136 (2003).
- [8] S. Kruger, S. Vent, F. Nortemann, M. Staufer, N. Rosch. The average bond length in Pd clusters Pd<sub>n</sub>, n=4–309: A density-functional case study on the scaling of cluster properties. *J. Chem. Phys.*, **115**(5), 2082 (2001).
- [9] A.P. Sutton, J. Chen. Long-range Finnis–Sinclair potentials. *Phil. Mag. Lett.*, **61**, 139 (1990).
- [10] H. Raffii-Tabar, A.P. Sutton. Long-range Finnis–Sinclair potentials for f.c.c. metallic alloys. *Phil. Mag. Lett.*, **63**, 217 (1991).
- [11] W. Smith, T.R. Forester. *DL\_POLY*, Daresbury Laboratory, Daresbury (1996).
- [12] M.P. Allen, D.J. Tildesley. *Computer Simulation of Liquids*, Clarendon Press, Oxford (1986).